Extreme load alleviation using industrial implementation of active trailing edge flaps in a full design load basis

2016 J. Phys.: Conf. Ser. 753 042001

(http://iopscience.iop.org/1742-6596/753/4/042001)

Extreme load alleviation using industrial implementation of active trailing edge flaps in a full design load basis

Thanasis Barlas, Vasilis Pettas, Drew Gertz and Helge A Madsen

Technical University of Denmark, Department of Wind Energy, Aerodynamic Design, DTU Risø Campus, Fredriksborgvej 399, 4000 Roskilde

E-mail: tkba@dtu.dk

Abstract.

The application of active trailing edge flaps in an industrial oriented implementation is evaluated in terms of capability of alleviating design extreme loads. A flap system with basic control functionality is implemented and tested in a realistic full Design Load Basis (DLB) for the DTU 10MW Reference Wind Turbine (RWT) model and for an upscaled rotor version in DTU's aeroelastic code HAWC2. The flap system implementation shows considerable potential in reducing extreme loads in components of interest including the blades, main bearing and tower top, with no influence on fatigue loads and power performance. In addition, an individual flap controller for fatigue load reduction in above rated power conditions is also implemented and integrated in the general controller architecture. The system is shown to be a technology enabler for rotor upscaling, by combining extreme and fatigue load reduction.

1. Introduction

The size of wind turbines has been increasing rapidly over the past years. Rotors of more than 160m in diameter are already commercially available. Focusing on lowering the cost per kWh, new trends and technological improvements have been primary targets of research and development. One main focus is on developing new technologies, which are, among other, capable of considerably reducing fatigue loads on wind turbines. New concepts for dynamic load reduction are focusing on a much faster and localized load control, compared to existing individual blade pitch control, by utilizing active aerodynamic control devices distributed along the blade span [1]. Such concepts are generally referred to as smart rotor control, a term used in rotorcraft research, and investigated for wind turbine applications over the past years in terms of conceptual and aeroelastic analysis, small scale wind tunnel experiments, and field testing [2, 3, 4, 5, 6]. So far, results from numerical and experimental analysis mostly focusing on trailing edge flaps have shown a considerable potential in fatigue load reduction [7, 8]. Existing work has provided aeroelastic tools with the capability of simulating active flap configurations, however the extreme load alleviation capability has yet to be studied thoroughly. Although there has been some focus on extreme load alleviation [9, 10, 11], it has not been generally evaluated in a realistic industrial load basis.

The current work describes the aeroelastic simulation activities on the load alleviation potential of a trailing edge flap in a realistic setup, close to the industrial certification-type of simulations. The implementation, load basis and pre-/post-processing comprise a robust and concrete comparison of load alleviation concepts. Testing the performance and robustness of the smart blade technology is an important part of the INDUFLAP2 project. Previous work has shown considerable potential in fatigue load reduction [1] and development of prototype flap systems [5]. A big step from prototype testing to full scale turbine application is a realistic evaluation of the load alleviation potential of such a system in conditions close to industrial standards. The load alleviation potential of using active flaps on wind turbine rotors has been investigated in the past decade using various models, controllers, configurations and load cases. In this work, the aeroelastic load simulations present a first approach for documenting such an evaluation on an overall realistic setup with basic flap control strategies.

2. Model and design load basis

The DTU 10MW RWT [12] is used for the simulations in the aeroelastic code HAWC2 [13], as a representative modern multi-MW wind turbine model which has been used extensively for comparison studies involving blade aerodynamic controls. Furthermore, a 5% increased blade length upscaled version of the reference rotor is modeled, which delivers 3.4% increased Annual Energy Production (AEP), with increase in most of the design loads, as evaluated in a full IEC DLB [14]. Specifically, ultimate blade root flapwise moment is increased by 19%, tip clearance by 10%, and tower bottom fore-aft moment by 12%. Blade root flapwise moment fatigue lifetime load is increased by 10%. The aerodynamic and structural characteristics of the blade have been kept the same at the relative blade positions. The 5% rotor is chosen as a the most realistic upscaling for this study, where the active flaps can deliver adequate load reduction for a load neutral upscaling. The power curve comparison of the upscaled rotor (5% and 10%) compared to the baseline is shown in Fig. 1. The figure also shows the effect of the peak thrust constraint which was used in order to deliver a realistic upscaled rotor for the existing wind turbine platform by forcing the upscaled turbines limit of the maximum steady state thrust to the level of the original rotor by introducing earlier pitch scheduling. The simulated flap configuration is chosen based on prior studies [8] and covers 30% of the blade length, starting from the tip, with 10% chordwise length. Allowed flap angles range between -15/+15 degrees.

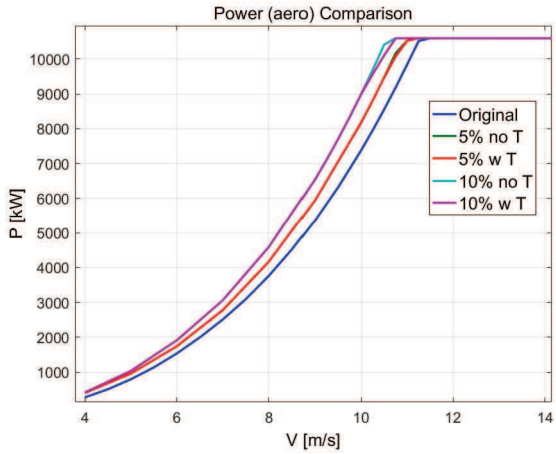

Figure 1. Comparison of power curves between the baseline and upscaled rotors by 5% and 10%.

The utilized DLB follows the current design standard (third edition of the IEC 61400-1) and is representative of a general DLB used by the industry in a certification process. The overview of the parameters defining the Design Load Cases (DLC) is presented in [14].

The standard DTU Wind Energy Design Load Case post-processing method for the DLB has been utilized. The procedure and algorithms applied are described in detail in [15]. This includes the process of extraction of the defined load sensors statistics, the ultimate (extreme value) analysis including the prescribed safety factor, and the fatigue analysis. Representative load sensors on the main components of the wind turbine aeroelastic model are chosen, with the corresponding parameters for fatigue analysis. The pitch bearing damage is also calculated, together with the pitch and flap activity.

The unsteady aerodynamics associated with the active flaps is accounted for by using the ATEFlap dynamic stall model in HAWC2 [16, 8]. The variation of steady lift, drag, and moment coefficients introduced by the flap deflection is based on 2D CFD simulations performed with the code Ellipsys2D [17]. The actuator dynamics are implemented as a linear servo model in HAWC2, for a first order system with a range of time constants simulating characteristics of various flap systems like the Controllable Rubber Trailing Edge Flap (CRTEF) actuators [5], or more modern basic industrial implementations.

3. Controller

The flap controller employs a basic cut-off strategy based on measurements of blade root flapwise moments, which is considered very close to industrial application capabilities being a simplistic and robust algorithm. The extreme blade flapwise moment statistics for normal power production cases (DLC group 1.x) and fault cases (DLC group 2.x) as defined by IEC standards and presented in [14] are shown in Fig. 2 and Fig. 3, respectively.

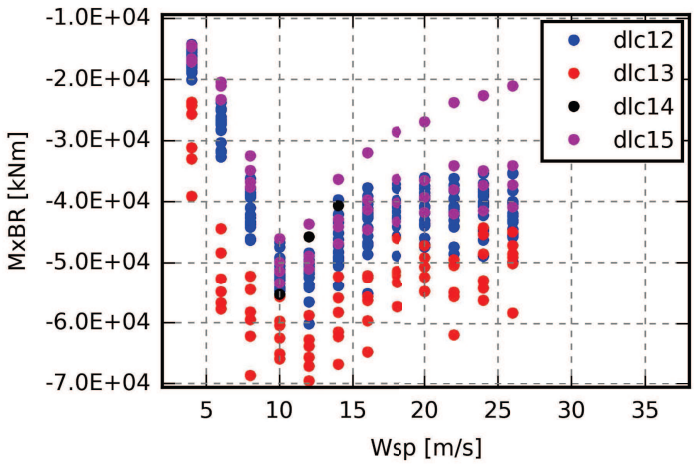

Figure 2. Extreme blade flapwise moment statistics for normal power production cases including safety factors (DLC group 1.x). 5% rotor with active flap control.

The objective of the controller is to bring the extreme blade load at the fault cases as close as possible to the normal power production with normal turbulence (DLC 1.2) levels, aiming at the reduction of ultimate design loads. The control operates such that when a flapwise root moment (MxBR) threshold is reached in any of the blades, then all three flaps are switched collectively to a prescribed target, following the actuator dynamics response, leading to instantaneous lift reduction. The flaps switch back to zero angle when all MxBR inputs are below the threshold.

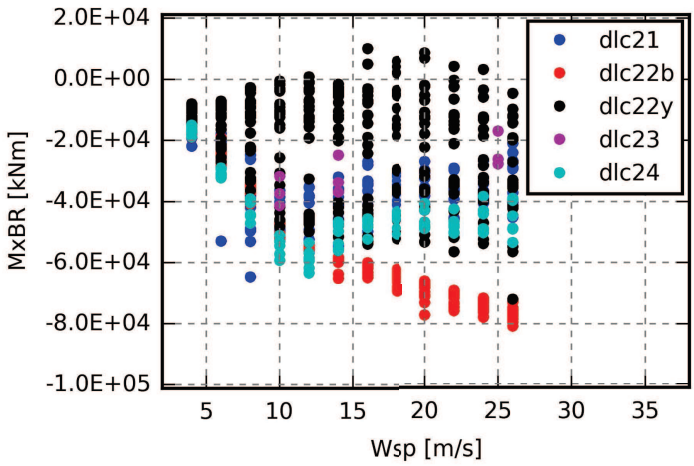

Figure 3. Extreme blade flapwise moment statistics for fault cases including safety factors (DLC group 2.x). 5% rotor with active flap control.

The threshold, the actuator dynamics as well as the behavior in parked cases were determined based on parametrical studies of the full DLB. Results showed a strong correlation between actuator dynamics (represented as a first order LP filter's time constant) and the threshold. The optimal values where selected so that the cut off controller is not activated during DLC 1.2, thus not affecting power production. For parked cases (DLC 6.x) a second lower threshold was implemented in order to reduce more effectively the occurring extreme loads. The extreme load flap controller architecture is shown in Fig. 4.

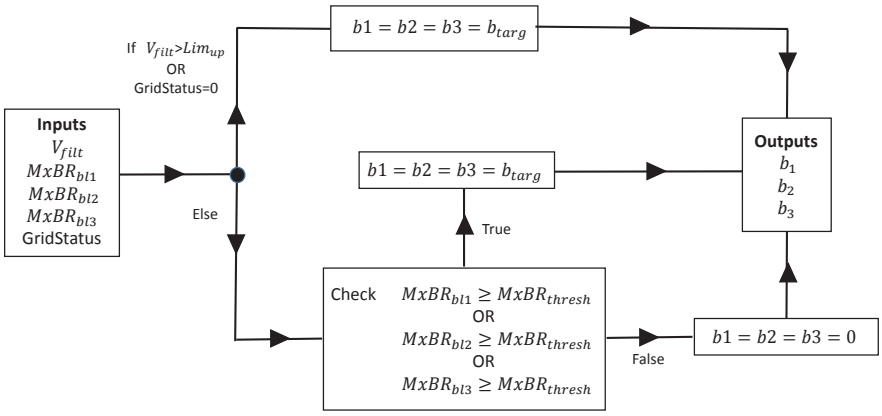

Figure 4. Collective flap cut-off extreme load controller architecture.

In addition, an individual flap feedback Proportional Derivative (PD) controller is employed, targeting the fatigue load reduction in above rated power conditions [18]. This is based on the observation that the lifetime fatigue in most of the channels is mainly contributed in full load conditions. The input of the controller is again the flapwise root bending moment with the flap action aiming to reduce magnitude and fluctuations of loads. A high pass filter is used

on the input signal in order to force the controller not to react to steady and low frequency variations. The PD gains are roughly tuned initially, using a closed loop state-space linearized representation of the system. Optimal values for gains as well as actuator's time constant were identified through parametrical studies on DLC 1.2, which is the design case contributing mostly in lifetime fatigue. The fatigue controller is decoupled from the extreme load controller based on the difference of threshold envelopes. Fatigue part is only active until a flap root moment threshold defined by the load envelope of DLC 1.2 and after that (meaning that the turbine experiences conditions other than normal power production) only the extreme load control is active. The fatigue load flap controller architecture is shown in Fig. 5.

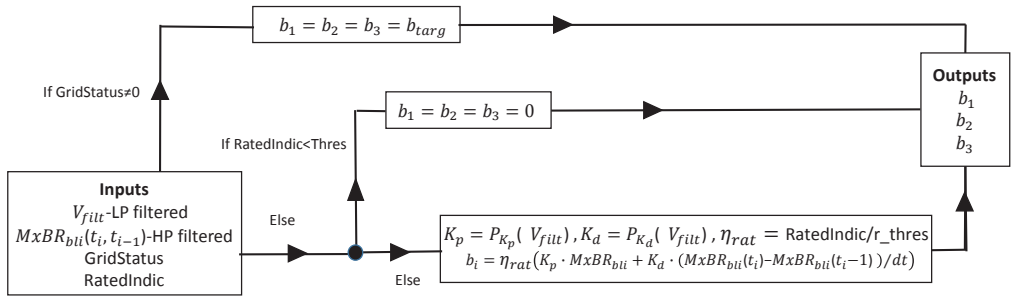

Figure 5. Individual flap PD fatigue load controller architecture

4. Results

Application of the extreme load controller on the baseline model shows a considerable extreme load alleviation in various load channels of interest, including the blades, main bearing and tower top (abbreviations of load channels shown in Table 1). The comparison of overall load level for ultimate loads is shown in Fig. 6, and in Table 2 with also the corresponding load cases of occurrence. The controller enables the use of the flap system solely in the case of extreme load exceedance. A representative time series of the blade root flapwise moment signal and the flap angle is shown in Fig. 7. The proposed method using an ATEFlap system with a cut-off switch control approach is found to be effective in ultimate loads alleviation. The main impact is observed on flapwise and edgewise blade root moments, tip clearance, nacelle roll and yaw moments as well as the main bearings yaw moment. Tower-related and nacelle tilt moment channels showed incremental decrease while main bearings yow moment and torsion, and blade root torsion are slightly increased. Furthermore, this control approach has no impact on fatigue and AEP as the full DLB simulations showed. From the investigations of the controllers parameters some conclusions can be derived. Firstly, regarding the load alleviation mechanism of the controller: Load alleviation potential is mainly limited by the dynamics of the system rather than the effective change in Cl. As observed in most cases, the peak load occurs when the cut-off is already activated. This shows that the dynamic effect of the fast change in flap angle (and consequently local Cl and lift) affected mainly by the combination of thresholds and servos time constant choices, and wind inflow dynamics is the dominant one. It is observed that after a point the total instantaneous decrease in aerodynamic forces (the longer the flap the highest the decrease) is not followed by a decrease in loads. When the transient phenomena induced by the

fast flap motion settle down the influence is decreased not allowing for further reduction. This explains, to an extent, why the fatigue oriented methods introduced so far are not so effective in extreme reduction. When the flap already follows the pattern of MxBR (or any other sensor relative to measured loads) flap angle is already decreased and the remaining dynamic margin is not enough to decrease further the peak loading.

Abbreviation	Load Channel
MxTB	Tower bottom fore-aft moment
MyTB	Tower bottom side-side moment
MxTT	Tower top tilt moment
MyTT	Tower top roll moment
MzTT	Tower top yaw moment
MxMB	Main bearing tilt moment
MyMB	Main bearing yaw moment
MzMB	Main bearing torsion
MxBR	Blade root flapwise moment
MyBR	Blade root edgewise moment
MzBR	Blade root torsion

Table 1. Abbreviations of the load channels considered.

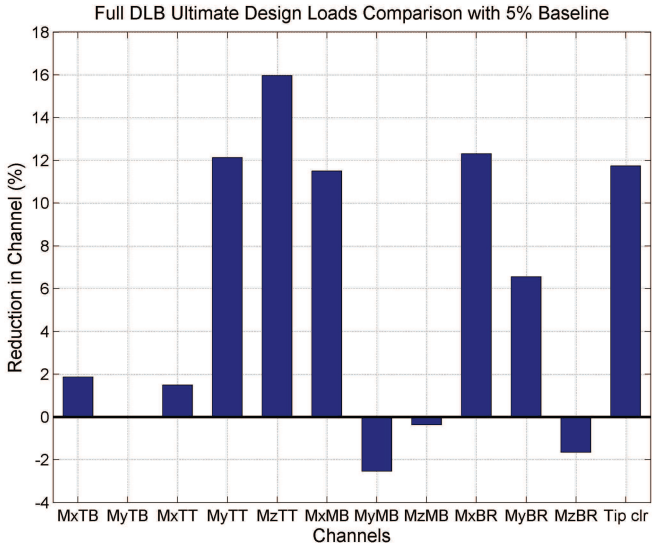

Figure 6. Reduction of ultimate design loads for different channels compared to no-flap case.

Application of the fatigue load controller on the baseline model shows a considerable lifetime fatigue load alleviation in various load channels of interest, including the blades, main bearing and tower top. The comparison of overall load level for fatigue loads are shown in Fig. 8. A representative time series of the blade root flapwise moment signal and the flap angle is shown in Fig. 9. The current implementation of the individual flap PD control based on HP filtered MxBR signals is shown to effect mainly blade root flapwise moment and main bearing channels and in a lower level tower base side-to-side moments while the other channels are

Name	Min incl. psf	Max incl. psf	DLC min	DLC max
MxTB	-4.30E+05	3.31E+05	22y_wsp26_wdir225_s7112	14_wsp10_wdir000_s0000
MyTB	-2.90E+05	2.95E+05	62_wsp50_wdir300_s9995	62_wsp50_wdir045_s9978
MxTT	-1.34E+05	1.20E+05	22b_wsp26_wdir000_s4012	22b_wsp26_wdir000_s6012
MyTT	-1.85E+04	3.38E+04	22y_wsp24_wdir195_s5111	81_wsp18_wdir008_s2108
MzTT	-1.29E+05	1.44E+05	22y_wsp24_wdir195_s5111	22y_wsp24_wdir195_s5111
MxMB	-1.08E+05	1.39E+05	22y_wsp26_wdir180_s4112	22b_wsp26_wdir000_s4012
MyMB	-1.06E+05	1.18E+05	22y_wsp24_wdir210_s6111	22y_wsp26_wdir210_s6112
MzMB	-8.32E+04	8.28E+04	22y_wsp26_wdir210_s6112	22y_wsp26_wdir210_s6112
MxBR	-9.18E+04	7.65E+04	22b_wsp26_wdir000_s4012	22y_wsp26_wdir240_s8112
MyBR	-8.63E+04	1.22E+05	22y_wsp24_wdir195_s5111	22y_wsp24_wdir195_s5111
MzBR	-1.21E+04	1.15E+04	22y_wsp26_wdir075_s6012	22y_wsp26_wdir270_s1212
TTDist	-9.79E-01	NAN	22b_wsp26_wdir000_s6012	-

Name	Min incl. psf	Max incl. psf	DLC min	DLC max
MxTB	-4.22E+05	3.31E+05	22y_wsp22_wdir210_s6110	14_wsp10_wdir000_s0000
MyTB	-2.95E+05	2.94E+05	62_wsp50_wdir315_s9996	62_wsp50_wdir060_s9979
MxTT	-1.32E+05	1.14E+05	22y_wsp24_wdir195_s5111	22b_wsp26_wdir000_s7012
MyTT	-1.97E+04	2.97E+04	22y_wsp24_wdir195_s5111	81_wsp18_wdir008_s2108
MzTT	-1.20E+05	1.21E+05	22y_wsp24_wdir195_s5111	22y_wsp24_wdir195_s5111
MxMB	-1.07E+05	1.23E+05	22y_wsp24_wdir165_s3111	22b_wsp26_wdir000_s4012
MyMB	-1.02E+05	1.21E+05	22y_wsp24_wdir195_s5111	22y_wsp26_wdir210_s6112
MzMB	-8.35E+04	8.29E+04	22y_wsp24_wdir210_s6111	22y_wsp24_wdir210_s6111
MxBR	-8.07E+04	7.73E+04	22b_wsp26_wdir000_s4012	22y_wsp26_wdir240_s8112
MyBR	-8.99E+04	1.14E+05	22y_wsp24_wdir195_s5111	22y_wsp24_wdir195_s5111
MzBR	-1.23E+04	1.15E+04	22y_wsp26_wdir075_s6012	22y_wsp26_wdir270_s1212
TTDist	-8.64E-01	NAN	22b_wsp26_wdir000_s4012	-

Table 2. Comparison of ultimate loads including DLC safety factors and corresponding load cases of occurrence. Upper-5% rotor without flaps, Lower-5% rotor with flaps.

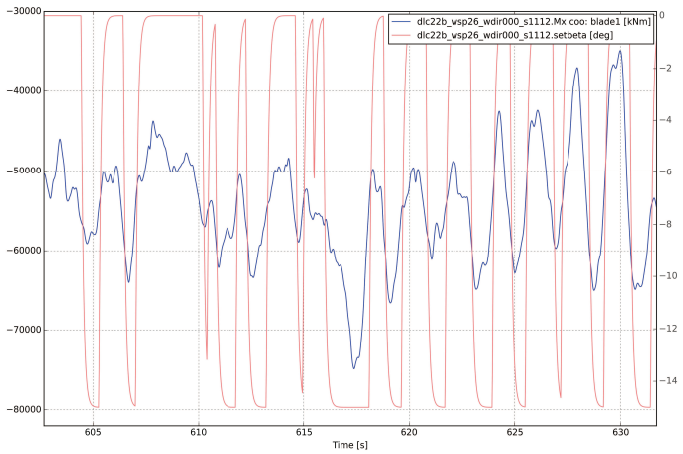

Figure 7. Representative time series for DLC2.2b at 26m/s with flap activity (red) and blade flapwise root moment signals (blue)-Extreme cut-off controller.

marginally affected towards decrease and blade torsion (as also observed in the ultimate load reduction investigations) is the only channel showing a significant increase of 8%. Regarding the objectives of a potential business case, the magnitude of decrease in the affected channels is close to the objectives though for the channels increased initially the most (MyBR and MzBR) no positive effect are observed. The analysis performed makes apparent the tradeoff between AEP and fatigue, since in order to further decrease fatigue loads, the controller has to be activated in speeds belonging in partial load regime. Moreover, the tradeoff between channels response is observed. After a poin,t by increasing the PD gains some channels showed an opposite effect by increasing load levels.

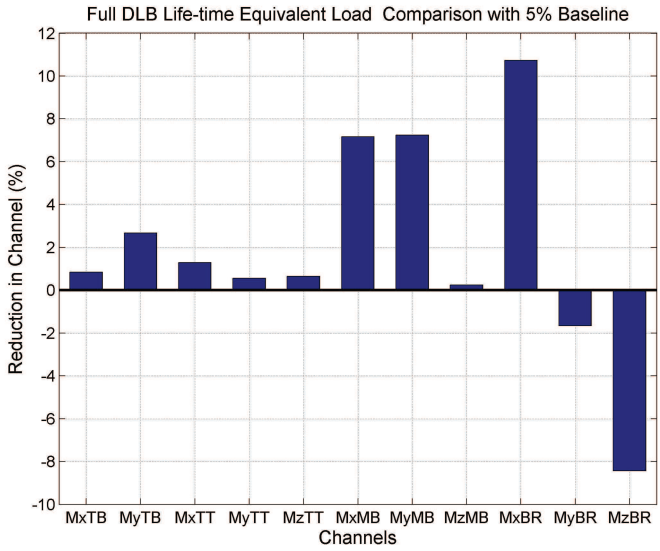

Figure 8. Reduction of lifetime fatigue loads for different channels compared to no-flap case.

5. Conclusion

The presented flap system implementation shows considerable potential in reducing extreme loads in components of interest including the blades, main bearing and tower, with additional reduction in fatigue loads and no influence on power performance. This is achieved in the 5% upscaled rotor with the active flap controllers, and load reduction is covering a large extent of the increased load levels in major components due to the upscaling from the baseline rotor. Specifically, ultimate blade root flapwise moment is reduced by 12% (19% increase in upscaling) and tip clearance by 12% (10% increase in upscaling), while blade root flapwise moment lifetime fatigue load is reduced by 11% (10% increase in upscaling). Thus, the system is shown to be a potential technology enabler for rotor upscaling. Further work could focus on more detailed evaluation of design loads (e.g. blade cross-sectional loads), and possible controller implementations having further impact on load increases in other relevant load channels.

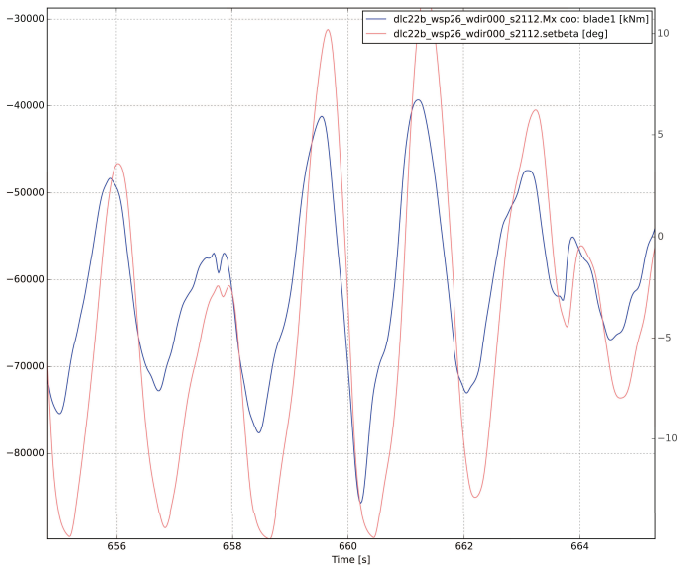

Figure 9. Representative time series for DLC1.2 at 26m/s with flap activity (red) and blade flapwise root moment signals (blue)-Fatigue controller.

Acknowledgments

The work has been funded by the Danish development and demonstration program EUDP under contract J.nr. 64015-0069 for the research project and research and development work *Full scale demonstration of an active flap system for wind turbines.*

References

[1] Barlas T. K. and van Kuik G. A. M. Review of state of the art in smart rotor control research for wind turbines *Progress in Aerospace Sciences* **46** 1 pp 1-27 2010

[2] Van Wingerden J. Hulskamp A. Barlas T. Houtzager I. Bersee H. van Kuik G. and Verhaegen M. Two-degree-of-freedom active vibration control of a prototyped 'smart' rotor *IEEE Transactions on Control Systems Technology* **19(2)** 284-296 2011

[3] Madsen HA. Andersen P. B., Andersen T. Bak C. and Buhl T. The potentials of the controllable rubber trailing edge flap (CRTEF) *Proceedings of EWEC 2010*, 20-23 April 2010, Warsaw, Poland

[4] Barlas T. K. and Madsen H. A. Influence of Actuator Dynamics on the Load Reduction Poetntial of Wind Turbines with Distributed Controllable Rubber Trailing edge Flaps (CRTEF) *Proceedings of ICAST2011: 22nd International Conference on Adaptive Structures and Technologies, October 10-12, 2011, Corfu, Greece* 2011.

[5] Madsen H. A. et al. Towards an industrial manufactured morphing trailing edge flap system for wind turbines *Proceedings of EWEC 2014, Barcelona, Spain* 2014

[6] Castaignet D. Barlas T. Buhl T. Poulsen N. K. Wedel-Heinen J. J. Olesen N. A. Bak C. and Kim T. Full-scale test of trailing edge flaps on a Vestas V27 wind turbine: active load reduction and system identification *Wind Energy* **17(4)** 549-564 2014.

[7] Barlas T. Active aerodynamic load control on wind turbine blades: Aeroservoelastic modelling and wind tunnel experiments *PhD thesis, TUDelft* 2011

[8] Bergami L. Adaptive Trailing Edge Flaps for Active Load Alleviation in a Smart Rotor Configuration *PhD thesis, DTU Wind Energy* 2013

[9] Lackner, M. A. and van Kuik, G. A. M. *Journal of Solar Energy Engineering* **132** 1 pp 12 2010

[10] Baek P. *Unsteady Flow Modeling and Experimental Verification of Active Flow ControlConcepts for Wind Turbine Blades*, PhD thesis, DTU Wind Energy, 2011

[11] Bernhammer L. O. et al. Fatigue and extreme load reduction of wind turbine components using smart rotors *Journal of Wind Engineering and Industrial Aerodynamics* **154** pp 84-95 2016

[12] Bak C. et al Description of the DTU 10 MW Reference Wind Turbine *Technical report, DTU Vindenergi-I-0092* 2013
[13] Larsen T. J. et al. How 2 Hawc2, the user's manual *Technical report, Risø-R-1597(ver. 4-4)(EN)* 2013
[14] Hansen M. H. et al. Design Load Basis for onshore turbines *Technical report, DTU Vindenergi-E-0174(EN)* 2015
[15] Hansen M. H. et al. Basic DTU Wind Energy controller *Technical report, DTU Vindenergi-E-0018(EN), Edition 2* 2015
[16] Bergami L. and Gaunaa M ATEFlap Aerodynamic Model, a dynamic stall model including the effects of trailing edge flap deflection *Technical report, Risø-R-1792(EN)* 2012
[17] Sørensen N. N. General purpose flow solver applied to flow over hills *Technical Report Risø-R-827(EN)* 1995.
[18] Barlas T. Load alleviation potential of the Controllable Rubber Trailing Edge Flap (CRTEF) in the INDUFLAP project *Technical report, DTU Vindenergi-E-0065(EN)* 2014